

## Supplementary Information

### Anthracene-arylamine hole transporting materials for perovskite solar cells

Xuepeng Liu,<sup>a,b</sup> Fantai Kong,<sup>\*a</sup> Rahim Ghadari,<sup>c</sup> Shengli Jin,<sup>d</sup> Ting Yu,<sup>a,b</sup> Wangchao  
Chen,<sup>a,b</sup> Guozhen Liu,<sup>a,b</sup> Zhan'ao Tan,<sup>d</sup> Jian Chen<sup>a</sup> and Songyuan Dai<sup>\*d,a</sup>

<sup>a</sup> Key Laboratory of Photovoltaic and Energy Conservation Materials, Institute of Applied Technology, Hefei Institutes of Physical Science, Chinese Academy of Sciences, Hefei, Anhui, 230088, P.R. China, Email: kongfantai@163.com

<sup>b</sup> University of Science and Technology of China, Hefei, 230026, P.R. China

<sup>c</sup> Computational Chemistry Laboratory, Department of Organic and Biochemistry, Faculty of Chemistry, University of Tabriz, 5166616471 Tabriz, Iran

<sup>d</sup> Beijing Key Laboratory of Novel Thin-Film Solar Cells, North China Electric Power University, Beijing, 102206, P.R. China, Email: sydai@ncepu.edu.cn

## Contents

Materials and Synthesis of HTMs

Device fabrication

Instrumentation

Fig. S1 The absorption spectra of in solution films

Fig. S2 Photoluminescence spectrum of compounds

Fig. S3 DFT calculations

Fig. S4 Hole-mobility measurements

Fig. S5 DSC curves

Table S1 Optical, electrochemical and hole mobility parameters

Fig. S6 AFM topographical images of HTM films

Fig. S7 steady-state PL study of perovskite/HTM bilayer

Fig. S8 Error bars of the devices with different HTMs

Table S2 Detailed device parameters of every sample for Fig. S8

Fig. S9  $J$ - $V$  curves measured by scan direction

Table S3 The detailed device parameters for Fig. S9

Fig. S10 Stability test of the devices

Table S4 Detailed device parameters for Fig. S10

Analysis of relative costs of HTMs

Table S5 Materials, quantities and cost for the synthesis of **A102**

Table S6 Estimated chemical synthesis cost

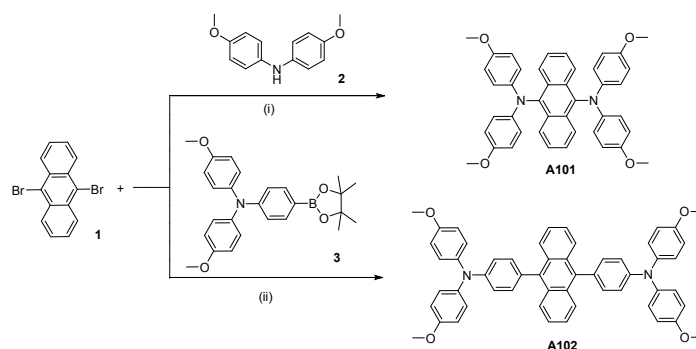
Fig. S11 The J-V curves of the CH<sub>3</sub>NH<sub>3</sub>PbI<sub>3</sub>-based solar cells

Table S9 Detailed device parameters for Fig. S11

Fig. S12-17 The <sup>1</sup>HNMR, <sup>13</sup>CNMR and HRMS

## 1. Materials and Synthesis of HTMs

All chemicals and reagents were purchased from TCI, Alfa, Sigma-Aldrich or Sinopharm Chemical Reagent Co.. Toluene was dehydrated by 4Å molecular sieves. Other chemicals were used as received with further processing. The final products are synthesized *via* Buchwald-Hartwig and Suzuki-Miyaura cross-coupling reaction, respectively. The detailed synthetic procedures of them are shown as follows.



**Scheme 1.** Synthetic routes for **A101** and **A102**. (i) *t*-BuOK, Pd(OAc)<sub>2</sub>, P(*t*Bu)<sub>3</sub>, toluene, reflux; (ii) K<sub>2</sub>CO<sub>3</sub>, Pd(PPh<sub>3</sub>)<sub>4</sub>, DMF, 90 °C.

**A101:** Compound **1** (0.69 g, 3 mmol), Compound **2** (0.47 g, 1.4 mmol), *t*-BuONa (0.96 g, 10 mmol), Pd(OAc)<sub>2</sub> (67 mg, 0.3 mmol), 30 mL anhydrous toluene, P(*t*-Bu)<sub>3</sub> (0.1 M in toluene, 0.3 mL) were added into a 100 mL flask and degassed using Ar. Then the reaction mixture is kept with stirring at 100 °C for 2 days. After cooling down, the reaction mixture is diluted by 50 mL dichloromethane (DCM) and washed with 60 mL water for 2 times. The organic phase is dried by NaSO<sub>4</sub>, then removed solvent using a rotary evaporator. The crude product is purified by column chromatography (DCM : PE = 1 : 2) to obtain the product as orange solid (0.73 g, 83%). <sup>1</sup>H NMR (400 MHz, DMSO) δ 8.12 (d, *J* = 6.3 Hz, 4H), 7.46 (d, *J* = 7.4 Hz, 4H), 6.91 (d, *J* = 8.0 Hz, 8H), 6.81 (d, *J* = 8.7 Hz, 8H), 3.67 (s, 12H). <sup>13</sup>C NMR (100 MHz, CDCl<sub>3</sub>) δ 153.95, 142.07, 137.62, 131.96, 126.48, 125.27, 121.22, 114.64, 55.53. HRMS (MALDI-TOF) *m/z*: [M-H] calcd 632.27; found 632.22.

**A102:** Compound **1** (0.27 g, 0.8 mmol), compound **3** (0.74 g, 1.8 mmol), Pd(PPh<sub>3</sub>)<sub>4</sub> (58 mg, 0.5 mmol), DMF (15 mL) and 2 M K<sub>2</sub>CO<sub>3</sub> (3 mL) were added into a 50 mL flask and degassed using Ar. The reaction mixture is stirred at 90 °C overnight. After cooling down, the reaction mixture is poured into cold Na<sub>2</sub>SO<sub>4</sub> aqueous solution, and crude product precipitate out as solids. The crude product is purified by column chromatography (DCM : PE = 1 : 2) to obtain the product as a yellow solid (0.77 g, 78%). <sup>1</sup>H NMR (400 MHz, DMSO) δ 7.74 (s, 4H), 7.45 (s, 4H), 7.23 (s, 12H), 7.01 (s, 12H), 3.78 (s, 12H). <sup>13</sup>C NMR (100 MHz, CDCl<sub>3</sub>) δ 156.01, 147.96, 140.96, 136.99, 131.89, 130.59, 130.29, 127.21, 126.95, 124.82, 119.85, 114.79, 55.53. HRMS (MALDI-TOF) m/z: [M-H] calcd 784.33; found 784.28.

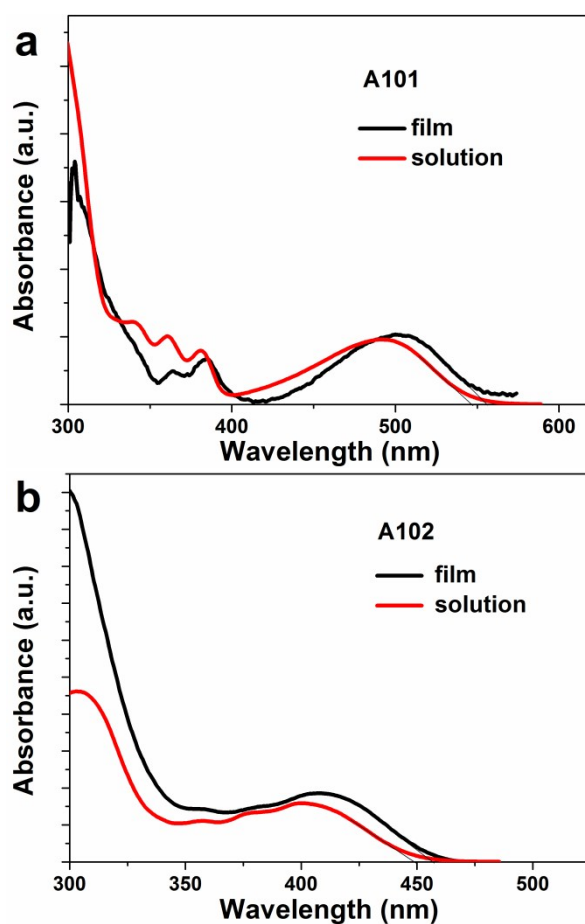
## 2. Device fabrication

FTO glass plates were sequentially cleaned by ultrasonic bath, water and ethanol. The compact TiO<sub>2</sub> layer was deposited on the etched substrate by spray pyrolysis at 450 °C using a precursor solution of 0.6 ml titanium diisopropoxide and 0.4 ml bis(acetylacetonate) in 7 ml anhydrous isopropanol. Mesoporous TiO<sub>2</sub> films was deposited on the substrate by spin-coating of a diluted particle TiO<sub>2</sub> paste (Dyesol 30NR-T, 1:5 w/w diluted in ethanol) at 5500 rpm for 20 s. Then the substrates were sintered at 510 °C for 30 min. After cooling down, The perovskite layer was deposited by spin-coating the perovskite precursor solution by a single step procedure. The perovskite precursor solution contained PbI<sub>2</sub> (1.1 M), FAI (1 M), PbBr<sub>2</sub> (0.2 M) and MABr (0.2 M) dissolved in a mixed solvent of DMF and DMSO solution (800 μl, volume ratio 1:4). The spin-coating procedure was carried out first 2000 rpm for 10 s, second 5000 rpm for 30 s. 90 μl chlorobenzene was poured on the spinning substrate during the second spin-coating step 15 s before the end of the procedure. The substrate was immediately heated at 100 °C for 1h on a hotplate. The HTM was subsequently deposited on the substrate by spin-coating at 4000 rpm for 20 s. The HTM solution were prepared in anhydrous toluene (**A101**: 12 mg mL<sup>-1</sup>, **A102**: 45 mg mL<sup>-1</sup>, spiro-OMeTAD: 73 mg mL<sup>-1</sup>) with 15 μL of 4-tert-butylpyridine, 8 μL of lithium bis(trifluoromethylsulphonyl)imide (520 mg mL<sup>-1</sup> in acetonitrile) and 6 μL (tris(2-(1H-pyrazol-1-yl)-4-tert-butylpyridine)cobalt(III) bis(trifluoromethylsulphonyl)imide solution (300 mg mL<sup>-1</sup> in acetonitrile). Finally, a ~60 nm thick Au counter electrode was deposited on top of the film by thermal evaporation.

## 3. Instrumentation

<sup>1</sup>H NMR and <sup>13</sup>C NMR spectra were carried out on a Brücker spectrometer (400 MHz) with chemical shifts against tetramethylsilane (TMS). Time-of-flight mass spectrometer (MALDI-TOF-MS) experiments were recorded using a MS Bruker Daltonik Reflex III and Bruker solariX spectrometer. The steady-state photoluminescence measurements were obtained from a Fluorescence Detector

(Fluorolog-3, HORIBA, USA) with a standard 450 W xenon CW lamp. Cyclic voltammetry was recorded on a CHI660d electrochemical analyzer (CH Instruments, Inc., China). A normal three electrode system was used and consisted of a platinum working electrode, a platinum wire counter electrode, and a calomel reference electrode. Redox potential of them was measured in DCM with 0.1 M tetrabutylammonium hexafluorophosphate with a scan rate of  $50 \text{ mV s}^{-1}$  (vs.  $\text{Fc}/\text{Fc}^+$  as an external reference). The UV-vis spectra were measured on a U3900H UV-Vis spectrophotometer (Hitachi, Japan). The current-voltage ( $J$ - $V$ ) characteristics of the PSC were carried out under AM 1.5 ( $100 \text{ mW cm}^{-2}$ ) illumination that was provided by a 3A grade solar simulator (Newport, USA, 94043A). The incident photon-to-current conversion efficiency (IPCE) was recorded on QE/IPCE measurement kit (Newport, USA). The morphologies of the samples were investigated by atomic force microscopy (5500 AFM (Agilent Technologies)).



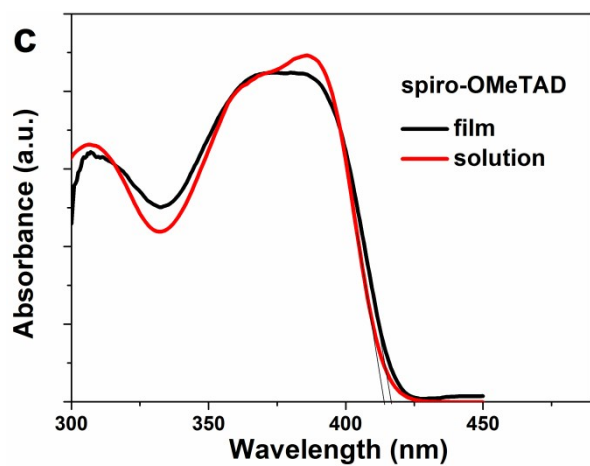


**Fig. S1** The absorption spectra of A101, A102, and spiro-OMeTAD in  $\text{CH}_2\text{Cl}_2$  solution and on glass films, respectively.

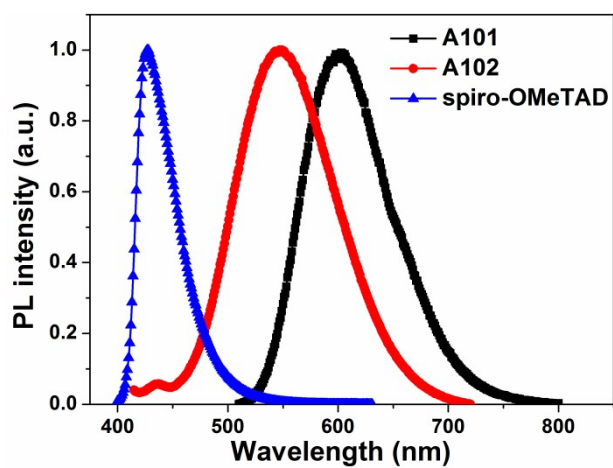


**Fig. S2** Photoluminescence spectrum of A101, A102 and spiro-OMeTAD in  $\text{CH}_2\text{Cl}_2$ .

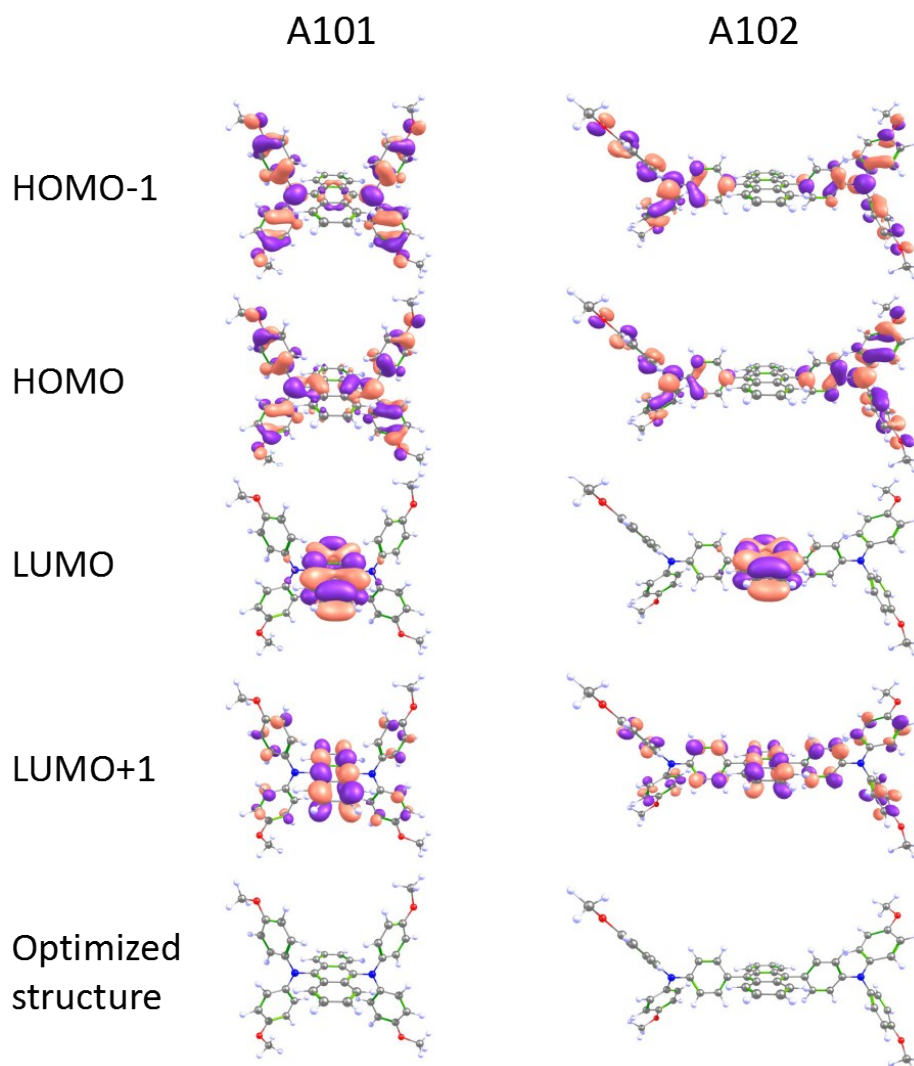


**Fig. S3** Geometry-optimized structures of the molecules and electron density distribution of the frontier molecular orbitals obtained from DFT calculations.

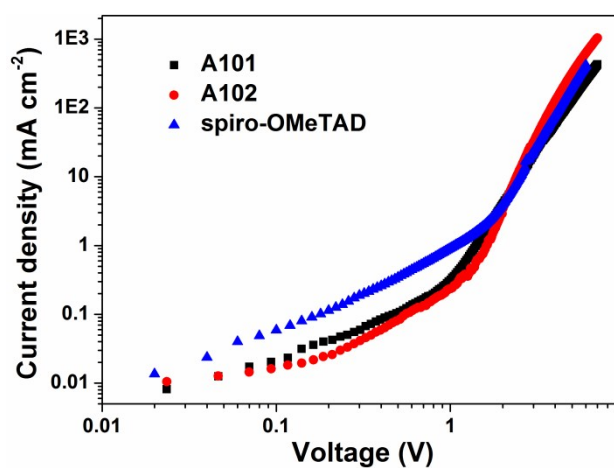


**Fig. S4** Hole-mobility measurements for A101, A102 and spiro-OMeTAD.

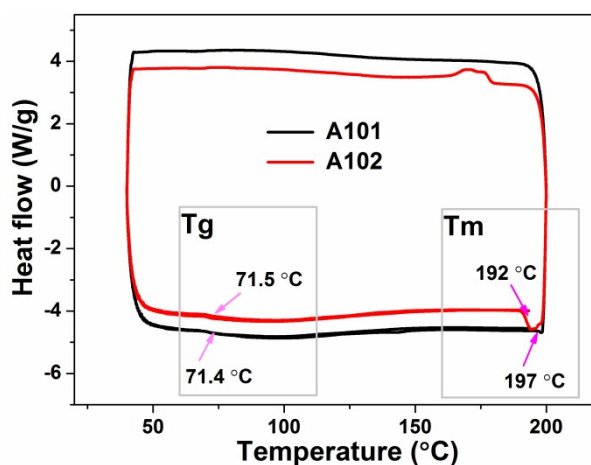


**Fig. S5** DSC curves of **A101** and **A102**.

**Table S1** Optical, electrochemical and hole mobility of synthesized HTMs.

| HTM                 | $\lambda_{\max}^{[a]}/\text{nm}$ | $E_g^{[b]}/\text{eV}$ | HOMO <sup>[c]</sup> /eV | LUMO <sup>[d]</sup> /eV | $M^{[e]}/\text{cm}^2\text{V}^{-1}\text{s}^{-1}$ |
|---------------------|----------------------------------|-----------------------|-------------------------|-------------------------|---|
| <b>A101</b>         | 491                              | 2.25                  | -5.26                   | -3.01                   | $7.85 \times 10^{-5}$                           |
| <b>A102</b>         | 401                              | 2.75                  | -5.31                   | -2.56                   | $9.02 \times 10^{-5}$                           |
| <b>spiro-OMeTAD</b> | 385                              | 2.98                  | -5.13                   | -2.15                   | $2.07 \times 10^{-5}$                           |

[a] UV-vis absorption spectra and emission spectra were measured in DCM solution. [b] (Optical band gap)  $E_g$  were estimated from UV absorption onset. [c] HOMO was calculated as  $E^{1/2}_{\text{ox}}$  vs.  $\text{Fc}/\text{Fc}^+ + 0.67$  vs. NHE + 4.44 vs. Vacuum. [d] LUMO = HOMO +  $E_g$ . [e]  $M$ : Hole mobility

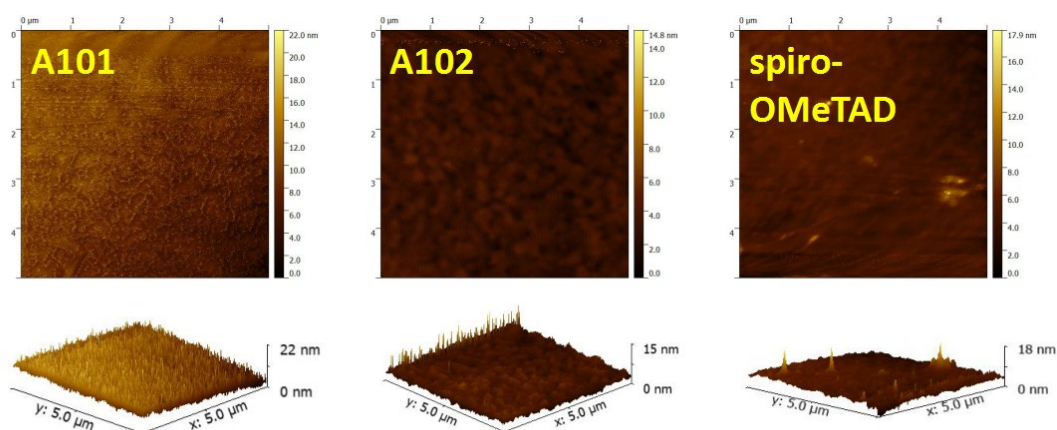


**Fig. S6** AFM topographical images of HTM films based on **A101**, **A102** and **spiro-**

OMeTAD

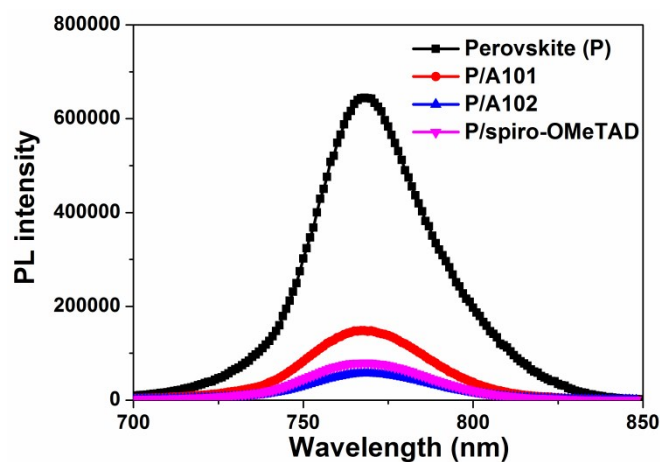


**Fig. S7** Steady state PL spectra of pristine perovskite and perovskite/HTM bilayer under excitation at 473 nm.

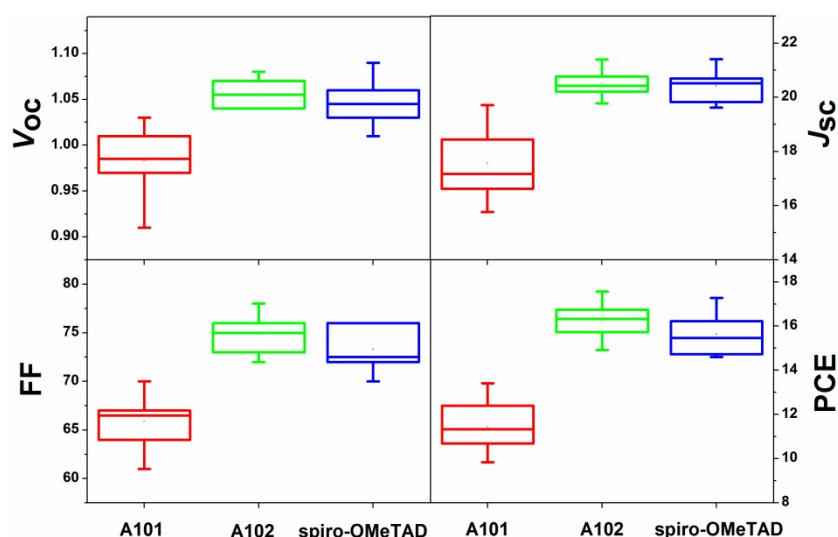


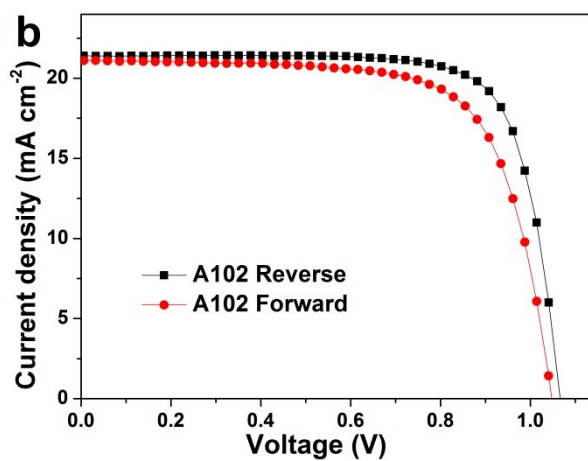
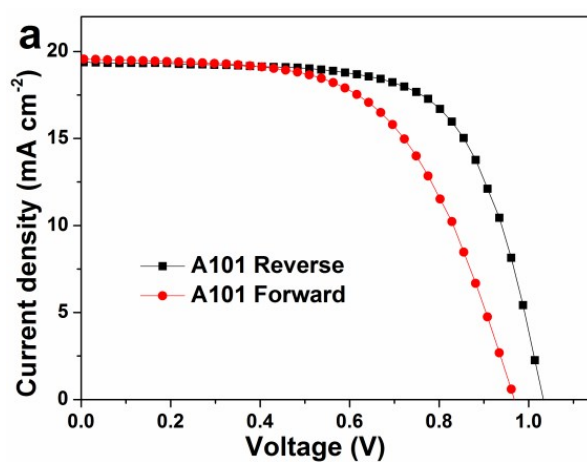
**Fig. S8** Power conversion efficiency (PCE), short-circuit current density ( $J_{sc}$ ), open-circuit voltage ( $V_{oc}$ ) and fill factor (FF) versus different HTMs. Error bars represent photovoltaic parameters deviations for the PSC devices employing A101, A102 or spiro-OMeTAD as HTM. Each group contains 10 independent samples.

**Table S2** Detailed device parameters of perovskite solar cells with different HTMs for Table 1 and Fig. S8.

| HTM  | Sample No. | $V_{oc}$ (V) | $J_{sc}$ (mA cm <sup>-2</sup> ) | FF (%) | PCE (%) |
|------|------------|--------------|---------------------------------|--------|---------|
| A101 | 1          | 1.01         | 16.76                           | 67     | 11.38   |

|                     |                   |                                |   |               |                |
|---------------------|-------------------|--------------------------------|---|---------------|----------------|
|                     | <b>2</b>          | 0.91                           | 18.44   | 63            | 10.68          |
|                     | <b>3</b>          | 0.95                           | 17.19   | 61            | 10.07          |
|                     | <b>4</b>          | 1.00                           | 16.54   | 69            | 11.44          |
|                     | <b>5</b>          | 0.99                           | 19.71   | 65            | 12.72          |
|                     | <b>6</b>          | 0.97                           | 15.77   | 64            | 9.84           |
|                     | <b>7</b>          | 1.03                           | 19.37   | 67            | 13.41          |
|                     | <b>8</b>          | 0.98                           | 17.15   | 66            | 11.04          |
|                     | <b>9</b>          | 1.02                           | 18.02   | 67            | 12.40          |
|                     | <b>10</b>         | 0.97                           | 16.62   | 70            | 11.27          |
|                     | <b>average</b>    | 0.99±0.03                      | 17.56±1.06                                      | 66±2.1        | 11.42±0.85     |
|                     | <b>Sample No.</b> | <b><math>V_{oc}</math> (V)</b> | <b><math>J_{sc}</math> (mA cm<sup>-2</sup>)</b> | <b>FF (%)</b> | <b>PCE (%)</b> |
| <b>A102</b>         | <b>1</b>          | 1.06                           | 20.50   | 73            | 15.91          |
|                     | <b>2</b>          | 1.04                           | 20.35   | 74            | 15.73          |
|                     | <b>3</b>          | 1.07                           | 20.56   | 75            | 16.48          |
|                     | <b>4</b>          | 1.04                           | 20.09   | 72            | 14.91          |
|                     | <b>5</b>          | 1.05                           | 20.76   | 75            | 16.50          |
|                     | <b>6</b>          | 1.07                           | 21.39   | 78            | 17.56          |
|                     | <b>7</b>          | 1.05                           | 19.77   | 73            | 15.17          |
|                     | <b>8</b>          | 1.04                           | 21.18   | 76            | 16.74          |
|                     | <b>9</b>          | 1.08                           | 20.21   | 78            | 17.03          |
|                     | <b>10</b>         | 1.06                           | 20.29   | 75            | 16.16          |
|                     | <b>average</b>    | 1.06±0.01                      | 20.59±0.37                                      | 75±1.54       | 16.22±0.64     |
|                     | <b>Sample No.</b> | <b><math>V_{oc}</math> (V)</b> | <b><math>J_{sc}</math> (mA cm<sup>-2</sup>)</b> | <b>FF (%)</b> | <b>PCE (%)</b> |
| <b>spiro-OMeTAD</b> | <b>1</b>          | 1.04                           | 20.95   | 75            | 16.22          |
|                     | <b>2</b>          | 1.01                           | 20.28   | 72            | 14.73          |
|                     | <b>3</b>          | 1.05                           | 20.69   | 70            | 15.22          |
|                     | <b>4</b>          | 1.05                           | 20.60   | 72            | 15.71          |
|                     | <b>5</b>          | 1.03                           | 19.82   | 72            | 14.73          |

|  |         |           |            |         |            |
|--|---------|-----------|------------|---------|------------|
|  | 6       | 1.02      | 19.64      | 73      | 14.60      |
|  | 7       | 1.06      | 19.62      | 76      | 15.77      |
|  | 8       | 1.09      | 20.56      | 76      | 16.96      |
|  | 9       | 1.04      | 20.47      | 71      | 15.14      |
|  | 10      | 1.06      | 21.40      | 76      | 17.27      |
|  | average | 1.04±0.02 | 20.40±0.45 | 73±1.79 | 15.63±0.75 |



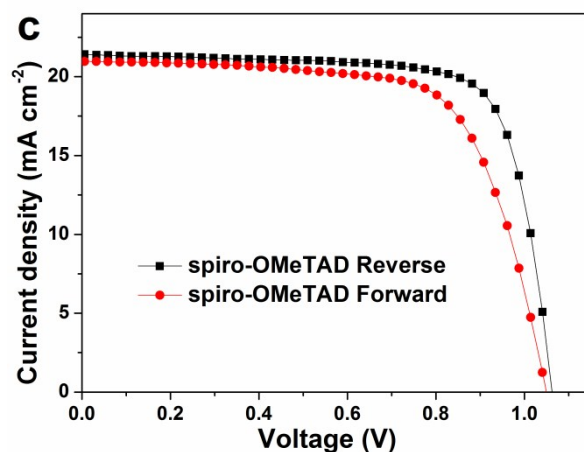


**Fig. S9**  $J$ - $V$  curves measured by forward scan (from short circuit to open circuit) and reverse scan (from open circuit to short circuit) of the PSCs with different HTMs under AM 1.5 illumination.

**Table S3** Summary of device parameters with different HTMs measured through forward and reverse scans for Fig. S9.

| HTM          |         | $V_{oc}$ (V) | $J_{sc}$ ( $\text{mA cm}^{-2}$ ) | FF (%) | PCE (%) |
|--------------|---------|--------------|----------------------------------|--------|---------|
| A101         | Reverse | 1.03         | 19.37                            | 67     | 13.41   |
|              | Forward | 0.97         | 19.56                            | 58     | 11.04   |
| A102         | Reverse | 1.07         | 21.39                            | 78     | 17.56   |
|              | Forward | 1.05         | 21.12                            | 71     | 15.64   |
| spiro-OMeTAD | Reverse | 1.06         | 21.40                            | 76     | 17.27   |
|              | Forward | 1.05         | 21.01                            | 70     | 15.31   |

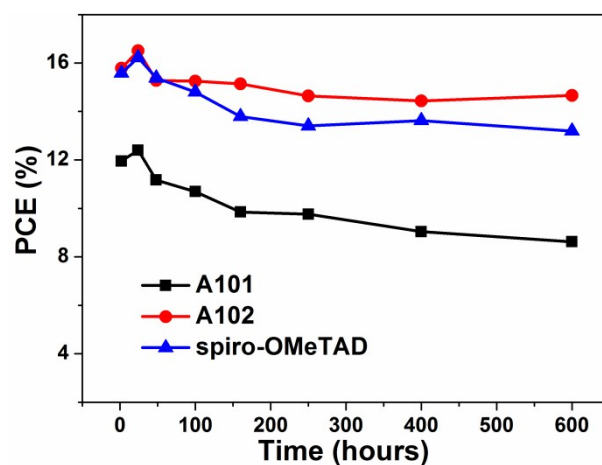


**Fig. S10** Stability test for the devices based on **A102** and spiro-OMeTAD.

**Table S4** The detail stability data of the devices with **A101**, **A102** or spiro-OMeTAD for Fig. S10.

|             | Time (hour) | $V_{oc}$ (V) | $J_{sc}$ (mA cm <sup>-2</sup> ) | FF (%) | PCE (%) |
|-------------|-------------|--------------|---------------------------------|--------|---------|
| <b>A101</b> | 2           | 1.02         | 17.73                           | 66     | 11.95   |
|             | 24          | 1.02         | 18.02                           | 67     | 12.40   |
|             | 48          | 0.98         | 17.76                           | 64     | 11.17   |
|             | 100         | 0.95         | 17.24                           | 65     | 10.69   |
|             | 160         | 0.96         | 16.81                           | 61     | 9.85    |
|             | 250         | 0.93         | 16.89                           | 62     | 9.76    |
|             | 400         | 0.94         | 15.98                           | 60     | 9.04    |
|             | 600         | 0.94         | 15.71                           | 58     | 8.62    |
| <b>A102</b> | 2           | 1.05         | 20.27                           | 74     | 15.78   |
|             | 24          | 1.05         | 20.76                           | 75     | 16.50   |
|             | 48          | 1.03         | 20.83                           | 71     | 15.28   |
|             | 100         | 1.06         | 20.82                           | 69     | 15.25   |
|             | 160         | 1.05         | 19.91                           | 72     | 15.14   |
|             | 250         | 1.05         | 20.22                           | 69     | 14.64   |
|             | 400         | 1.03         | 20.32                           | 69     | 14.43   |

|                     |     |      |       |    |       |
|---------------------|-----|------|-------|----|-------|
|                     | 600 | 1.04 | 19.99 | 71 | 14.66 |
| <b>spiro-OMeTAD</b> | 2   | 1.06 | 20.01 | 73 | 15.58 |
|                     | 24  | 1.04 | 20.95 | 75 | 16.22 |
|                     | 48  | 1.06 | 20.01 | 73 | 15.38 |
|                     | 100 | 1.04 | 19.97 | 71 | 14.80 |
|                     | 160 | 1.03 | 19.44 | 69 | 13.79 |
|                     | 250 | 1.03 | 19.50 | 67 | 13.40 |
|                     | 400 | 1.01 | 19.92 | 68 | 13.62 |
|                     | 600 | 1.03 | 19.35 | 66 | 13.19 |

### A simple analysis of relative costs of spiro-OMeTAD and A102

The lab synthesis cost of **A102** are estimated on a model originally proposed by Osedach *et al.*<sup>[1]</sup>. Recently, Pertrus and Malinauskas *et al.*<sup>[2,3]</sup> has used the model to estimate the cost of hole transporting materials. For every synthetic step the required amounts of reactants, catalysts, reagents and solvents are calculated to obtain 1 gram of **A102** are reported (Table S6).

**Table S5** Materials, quantities and cost for the synthesis of **A102**.

| Chemical  | Weight<br>Reagent or solvent<br>(g/g) | Price of<br>chemical<br>(RMB/g) | Cost of<br>chemical<br>(RMB/g product) | Total cost<br>(RMB/g) |
|---|---------------------------------------|---------------------------------|--|-----------------------|
| 4-methoxy-N-(4-methoxyphenyl)-N-(4-(4,4,5,5-tetramethyl-1,3,2-dioxaborolan-2-yl)phenyl)aniline <sup>[4]</sup> | 1.60                                  | 128                             | 205                                    |                       |
| Tetrakis(4-bromophenyl)methane  | 0.41                                  | 6.62<br>(adamas)                | 2.71                                   |                       |
| DMF   | 32                                    | 0.03                            | 0.96                                   |                       |
| Pd(PPh <sub>3</sub> ) <sub>4</sub>  | 0.12                                  | 72                              | 8.64                                   |                       |
| K <sub>2</sub> CO <sub>3</sub>  | 0.8                                   | 0.04                            | 0.032                                  |                       |
| Na <sub>2</sub> SO <sub>4</sub>   | 5                                     | 0.02                            | 0.1                                    |                       |
| CH <sub>2</sub> Cl <sub>2</sub>   | 450                                   | 0.03                            | 13.5                                   |                       |

|                 |     |      |     |     |
|-----------------|-----|------|-----|-----|
| Petroleum ether | 360 | 0.02 | 7.2 |     |
| <b>A102</b>     |     |      |     | 238 |

238 RMB/g = 34.6 \$/g

**Table S6** Survey of the estimated chemical synthesis cost for different HTMs

| compound     | Material cost (\$/g)   | Commercial price (\$/g)  |
|--------------|------------------------|--------------------------|
| <b>A102</b>  | 34.6                   | -                        |
| Spiro-OMeTAD | 91.67 <sup>[2,3]</sup> | 170-475 <sup>[2,3]</sup> |

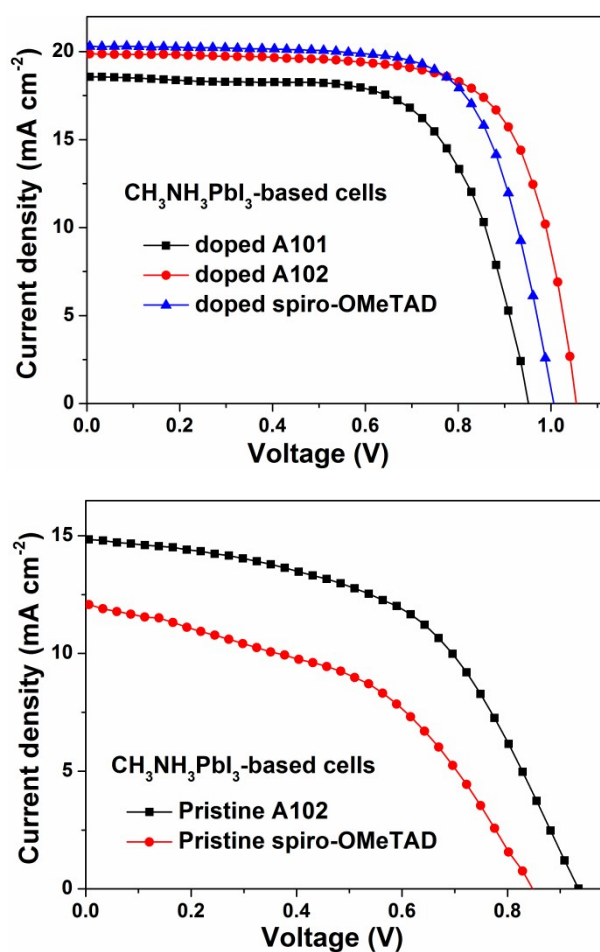


**Fig. S11** The  $J$ - $V$  curves of the CH<sub>3</sub>NH<sub>3</sub>PbI<sub>3</sub>-based solar cells employing doped or pristine A101, A102 or spiro-OMeTAD as HTM under AM 1.5 simulated sunlight.

**Table S7** Photovoltaic parameters of the CH<sub>3</sub>NH<sub>3</sub>PbI<sub>3</sub>-based solar cells obtained from  $J$ - $V$  curves of the corresponding devices for Fig. S11.

| HTM                   | $V_{oc}$ (V) | $J_{sc}$ (mA cm <sup>-2</sup> ) | FF (%) | PCE (%) |
|-----------------------|--------------|---------------------------------|--------|---------|
| Doped A101            | 0.95         | 18.58                           | 66     | 11.73   |
| Doped A102            | 1.05         | 19.88                           | 70     | 14.89   |
| Doped spiro-OMeTAD    | 1.01         | 20.29                           | 71     | 14.41   |
| Pristine A102         | 0.94         | 14.91                           | 52     | 7.22    |
| Pristine spiro-OMeTAD | 0.85         | 12.14                           | 46     | 4.69    |

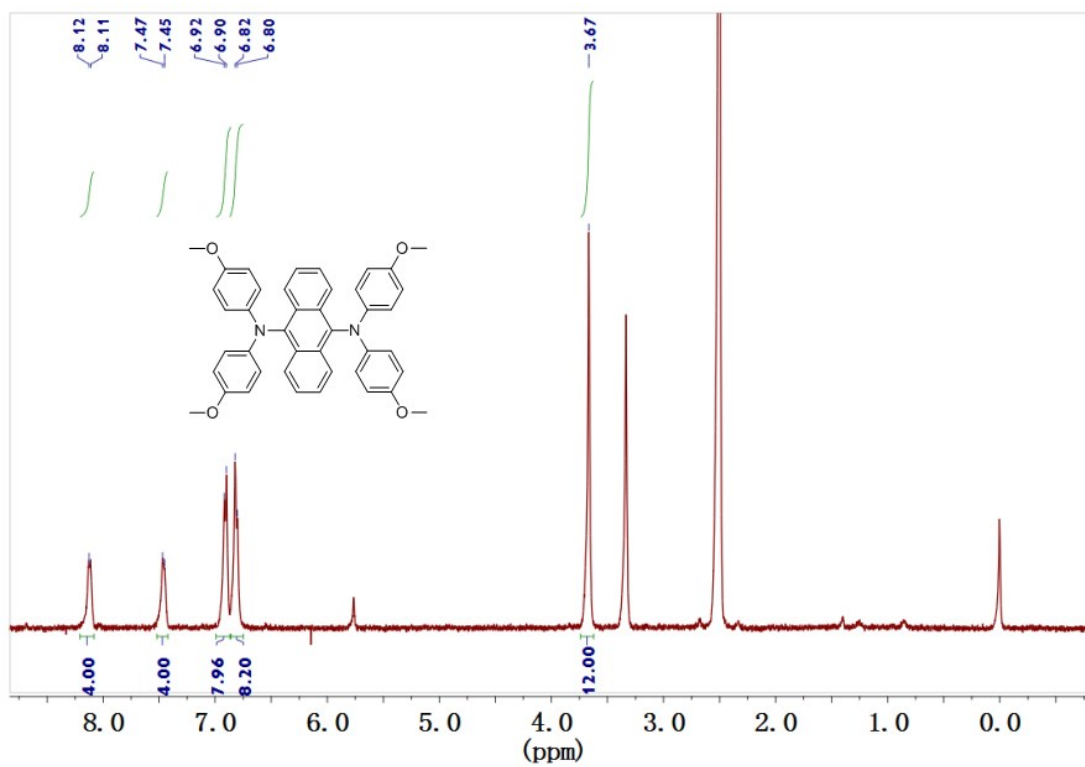


Fig. S12 <sup>1</sup>H-NMR of A101.

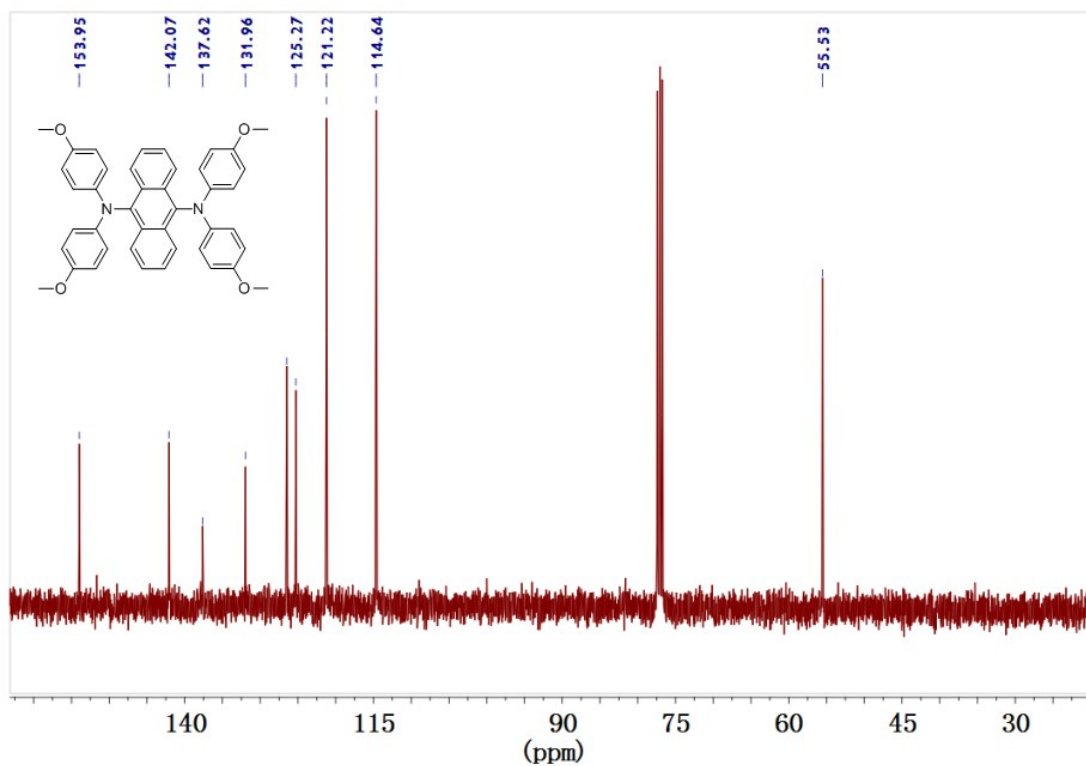
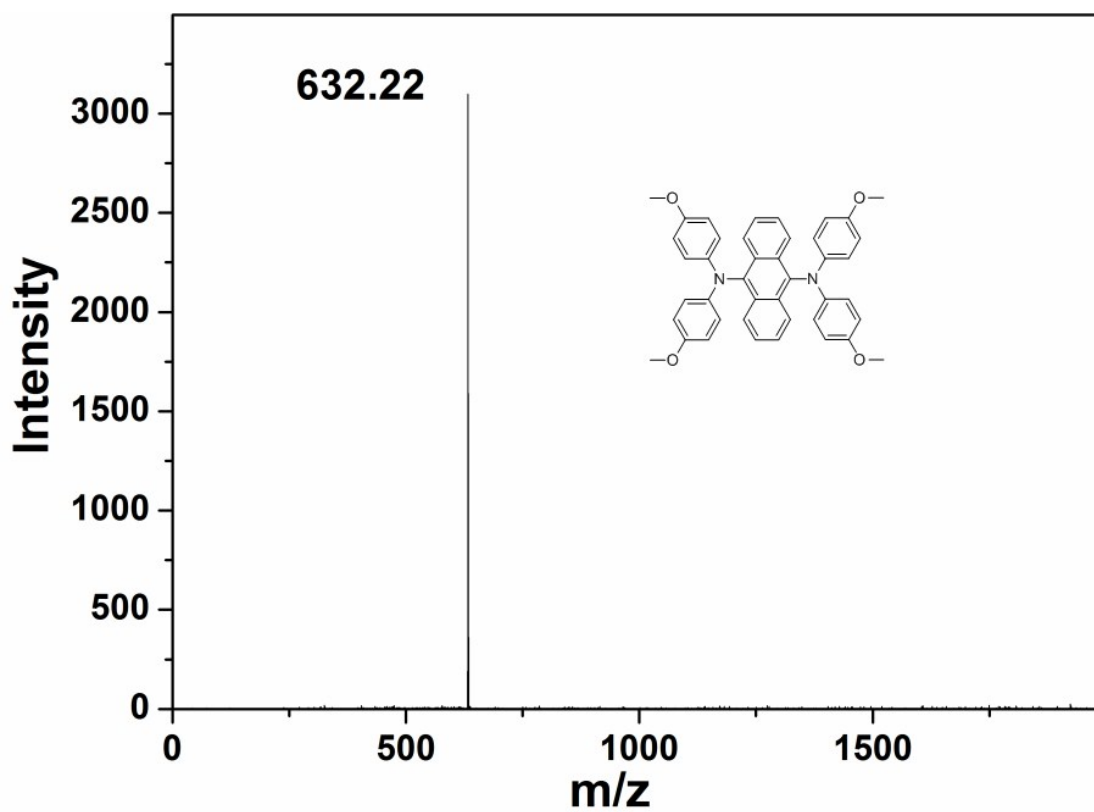
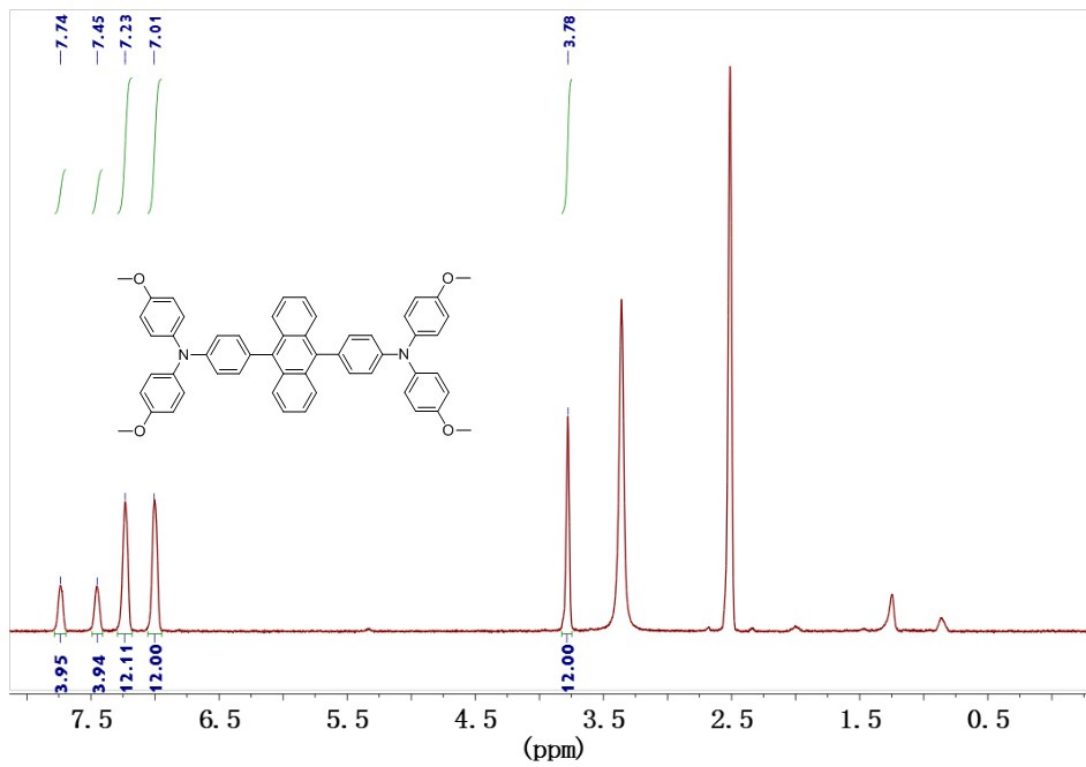


Fig. S13 <sup>13</sup>C-NMR of A101.



**Fig. S14** HRMS (MALDI-TOF) of **A101**.



**Fig. S15**  $^1\text{H-NMR}$  of **A102**.

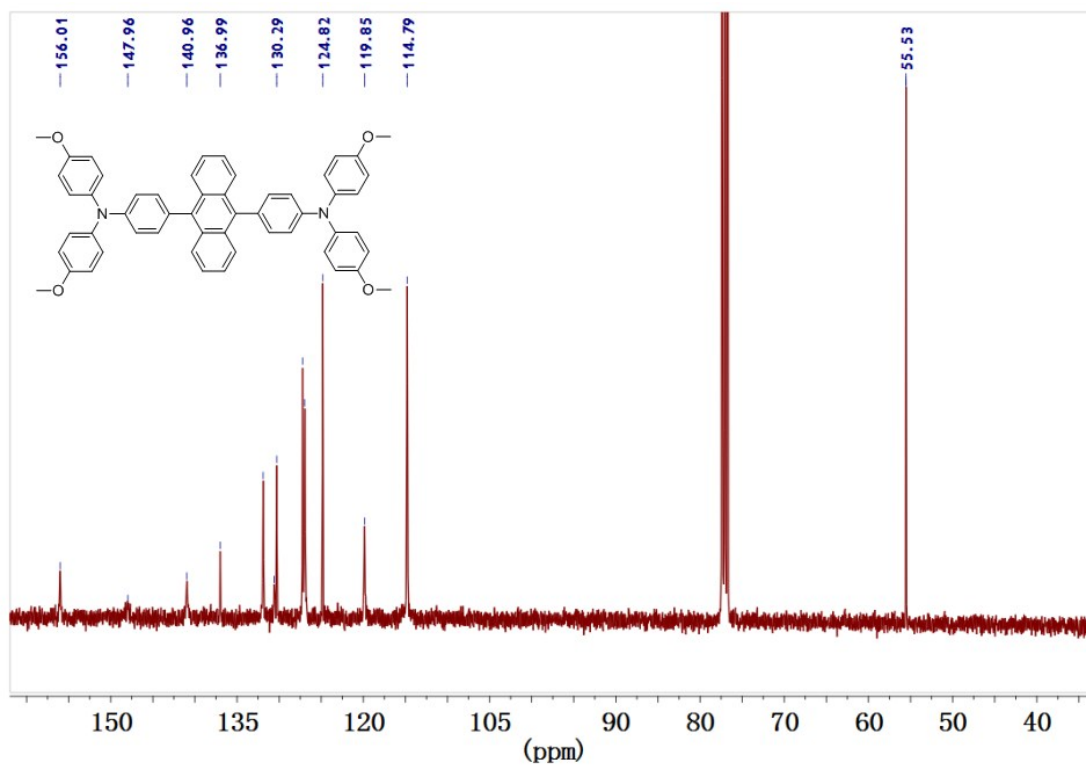


Fig. S16  $^{13}\text{C}$ -NMR of A102.

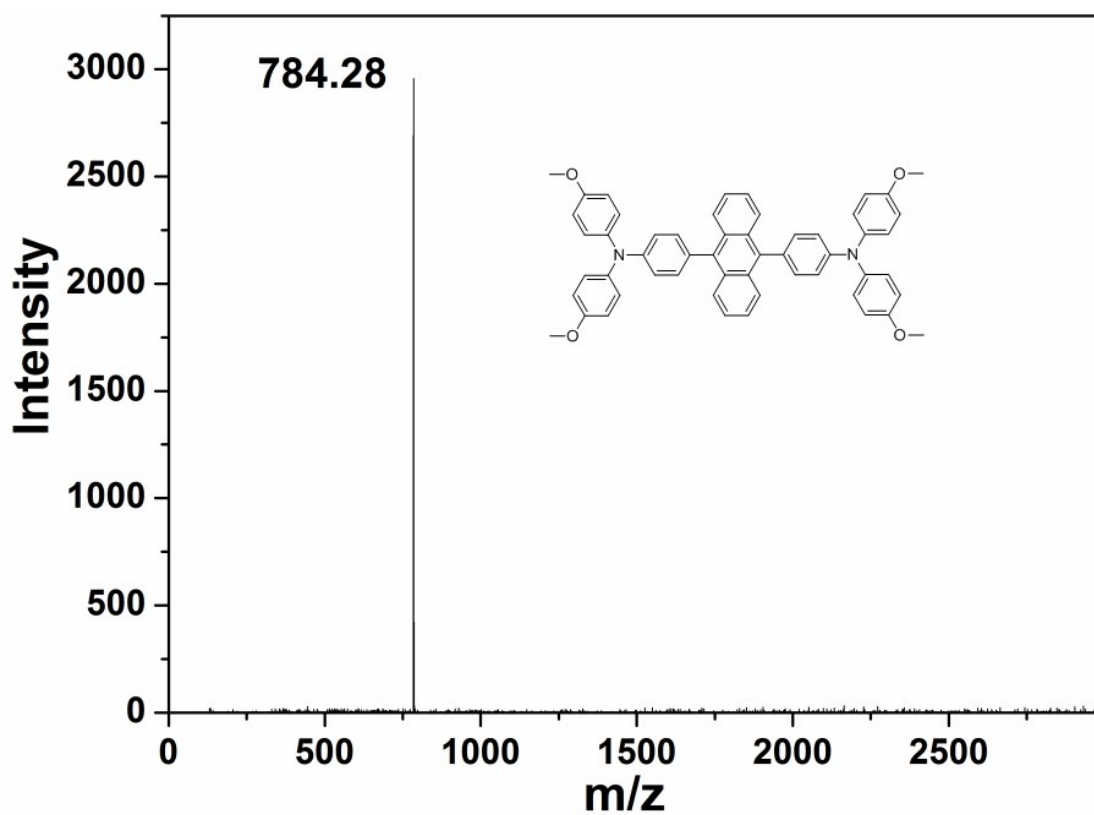


Fig. S17 HRMS (MALDI-TOF) of A102.

- [1] T. P. Osedach, T. L. Andrew, V. Bulovic, *Energ. Environ. Sci.*, **2013**, *6*, 711-718.
- [2] M. L. Petrus, T. Bein, T. J. Dingemans, P. Docampo, *J. Mater. Chem. A*, **2015**, *3*, 12159-12162.
- [3] T. Malinauskas, M. Saliba, T. Matsui, M. Daskeviciene, S. Urnikaite, P. Gratia, R. Send, H. Wonneberger, I. Bruder, M. Grätzel, *Energy Environ. Sci.* **2016**, *9*, 1681-1686.
- [4] X. Liu, F. Kong, T. Cheng, W. Chen, Z. Tan, T. Yu, F. Guo, J. Chen, J. Yao, S. Dai, *ChemSusChem*. **2017**, *10*, 968-975.